Automatic calibration of a large-scale sediment model using suspended sediment concentration, water quality, and remote sensing data

Calibração automática de um modelo hidrossedimentológico de grande escala usando dados de concentração de sedimentos em suspensão, qualidade da água e sensoriamento remoto

Hugo de Oliveira Fagundes[1] (ID)**, Fernando Mainardi Fan[1]** (ID)**, Rodrigo Cauduro Dias de Paiva[1]** (ID)

[1]Universidade Federal do Rio Grande do Sul, Porto Alegre, RS, Brasil
E-mails: h.o.fagundes@hotmail.com (HOF), fernando.fan@bol.com.br (FMF), rodrigocdpaiva@gmail.com (RCDP)

ABSTRACT

Calibration and validation are two important steps in the application of sediment models requiring observed data. This study aims to investigate the potential use of suspended sediment concentration (SSC), water quality and remote sensing data to calibrate and validate a large-scale sediment model. Observed data from across 108 stations located in the Doce River basin was used for the period between 1997-2010. Ten calibration and validation experiments using the MOCOM-UA optimization algorithm coupled with the MGB-SED model were carried out, which, over the same period of time, resulted in 37 calibration and 111 validation tests. The experiments were performed by modifying metrics, spatial discretization, observed data and parameters of the MOCOM-UA algorithm. Results generally demonstrated that the values of correlation presented slight variations and were superior in the calibration step. Additionally, increasing spatial discretization or establishing a background concentration for the model allowed for improved results. In a station with high quantity of SSC data, calibration improved the ENS coefficient from -0.44 to 0.44. The experiments showed that the spectral surface reflectance, total suspended solids and turbidity data have the potential to enhance the performance of sediment models.

Keywords: MGB-SED; Doce River; Erosion; MUSLE; Sediment modelling.

RESUMO

A calibração e a validação são duas etapas importantes na aplicação de modelos de sedimentos que requerem dados observados. Nesse contexto, este estudo investigou o potencial de uso dos dados de concentração de sedimentos em suspensão (CSS), qualidade da água e sensoriamento remoto na calibração e validação de um modelo hidrossedimentológico de grande escala. Foram usados dados observados de 108 estações, localizadas na bacia do rio Doce, para o período entre 1997 e 2010. Foram realizados dez experimentos de calibração e validação usando o algoritmo de otimização MOCOM-UA, acoplado ao modelo MGB-SED, resultando em 37 calibrações automáticas e 111 testes de validação, todos no mesmo período. Os experimentos foram construídos modificando as métricas, discretização espacial, dados de CSS e parâmetros do algoritmo MOCOM-UA. Os resultados mostraram que, no geral, os valores das correlações variaram pouco e foram melhores na etapa de calibração. Observou-se que, o aumento da discretização espacial da bacia ou o estabelecimento de uma concentração mínima para o modelo, possibilitou obter resultados melhores. Em uma estação com muitos dados de CSS, a calibração melhorou o coeficiente de ENS de -0,44 para 0,44. Os experimentos mostraram que os dados de refletância espectral de superfície, sólidos suspensos totais e turbidez apresentam potencial para melhorar a performance dos modelos de sedimentos.

Palavras-chave: MGB-SED; Rio Doce; Erosão; MUSLE; Modelagem de sedimentos.

INTRODUCTION

Monitoring suspended sediments (SS) in water bodies is useful in the development of various studies that relate sediments to environmental, social and economic issues (MORRIS; FAN, 1998). Through the use of observed data and sediment models it is possible to understand erosion processes and sediment transport; and to simulate scenarios which involve climactic alterations or land cover and land use, for example (MILLINGTON, 1986; MERRITT; LETCHER; JAKEMAN, 2003; SANTOS, 2009; PANDEY et al., 2016; WORKU; KHARE; TRIPATHI, 2017).

Two important procedures to applicate sediment models are calibration and validation, which aim to ensure their optimal performance (BRESSIANI et al., 2015; PANDEY et al., 2016). Bressiani et al. (2015) demonstrated that calibration is only performed in 66% of the models in Brazil in order to achieve improved results. Model calibration is commonly carried out manually, adjusting the parameters through trial and error, turning it into a very time consuming and monotonous task (SUGAWARA, 1979; BOYLE; GUPTA; SOROOSHIAN, 2000; MULETA; NICKLOW, 2005). However, in order to achieve a satisfactory fit between observed and simulated data, a learning period is necessary. This arises from the lack of knowledge regarding the exact outcome of changes in parameters values in each region of the model application. One's insights acquired through practice is difficult to be swiftly transferred to another person, let alone to another model (BOYLE; GUPTA; SOROOSHIAN, 2000). To aid the user in applying a model - which does not exempt them from having basic knowledge about the basin's physical characteristics, the model and its parameters - optimization methods and algorithms (e.g. YAPO; GUPTA; SOROOSHIAN, 1998; VRUGT et al., 2003; MULETA; NICKLOW, 2005) were implemented in hydrological (e.g. GUPTA; SOROOSHIAN; YAPO, 1998; VINEY; SIVAPALAN, 1999; BOYLE; GUPTA; SOROOSHIAN, 2000; TUCCI; COLLISCHONN, 2003; BLASONE; MADSEN; ROSBJERG, 2007; TUCCI; BRAVO; COLLISCHONN, 2009) and sediment (see Table 1) models, allowing for the parameters calibration automatically. Few sediment model studies were carried out using automatic calibration (Table 1). The main goals of the studies displayed on Table 1 were: to calibrate, to analyze uncertainties and to validate models; to compare the performances of different models; and to compare automatic calibration methods.

Among them, the studies of Van Rompaey et al. (2005) and Rostamian et al. (2008) Respectively grant that automatic calibration can be used to perform a various number of experiments (simulations), and to perform applications in large basins. A problem that emerges in merging these two approaches is that calibration and validation procedures demand observed data, of which suspended sediment concentration (SSC) or discharge (QSS) are normally used. On the other hand, we verify a low density of measuring stations across monitoring networks, few of them presenting long and continuous series of data (LODHI et al., 1998; PANDEY et al., 2016). According to Pandey et al. (2016), this limits the understanding of erosion ratios in the multiple spatial and temporal scales, as well as that of the efficiency of erosion control measures.

In face of these issues, several alternatives to standard monitoring have been developed to estimate suspended sediments (SS), based on water quality data or spectral surface reflectance (SSR), obtained from Remote Sensing images (RS). Glysson, Gray and Conge (2000) and Williamson and Crawford (2011) used total suspended solids (TSS) data to estimate SSC through linear regression. Pavanelli and Bigi (2005) and Minella et al. (2008) estimated SSC from turbidity data through empirical equations developed over each Rspective study. Sari, Castro and Pedrollo (2017) imputed turbidity data in a artificial neural networks model and secured valuable SSC estimations. SSR data has been used to undertake SS estimations in water bodies since the deployment of the Landsat 1 satellite, as exposed by Munday Junior and Alföldi (1979). Lodhi et al. (1998) carried out a laboratory study concerning the relationship between SSC and SSR data across different concentrations. Martinez et al. (2009) and Espinoza Villar et al. (2012) also developed empirical equations to estimate SSC from SSR in the Amazon, and Ucayali and Marañon (Amazon's tributaries) rivers, Respectively. Zhang et al. (2014) carried out procedures similar to those of Martinez et al. (2009) and Espinoza Villar et al. (2012), to estimate SSC in the Huang He (Yellow River) estuary.

Despite the aforementioned studies employing RS to estimate SSC, none have broached the matter of using these information to calibrate models. Miller et al. (2005) and Yang et al. (2014) used SSC derived data from satellite images to calibrate and validate sediment transport models for coastal waters. These two were the few studies in the literature that were found which used RS to calibrate or validate a sediment transport model.

The advantage of using surrogate data sources, be it water quality or RS data, comes from increasing the availability of information stemming from such indirect measurements, which broadens the monitoring scope. Within the context of large-scale sediment modeling, however, a few limitations and disadvantages are made present through the sole use of SSC derived from empirical equation (such as those used by Miller et al. (2005) and Yang et al (2014)): (i) in order to establish these relationships in an accurate manner, a sufficiently long SSC series is necessary that be representative of the basin conditions both in dry and in wet seasons; (ii) generally, these relationships are only reasonable over the location where the station was deployed; (iii) in many regions, the spatial density of water quality data stations and virtual stations (created from remote sensing images) is much higher than that of sediment stations. Thus, being limited to the use of sediment data derived from empirical equations would be to waste alternative information which have great application potential in studies related to sediment transport.

No research within the literature, however, has been found to directly use water quality and RS data in automatically calibration a sediment model at a basin-scale. Therefore, there are no clear recommendations regarding how to handle such data. In face of this context, the present study investigated the potential use of SSC, turbidity, total suspended solids and spectral surface reflectance data to calibrate and validate a large-scale sediment model. To that end, the MOCOM-UA (YAPO; GUPTA; SOROOSHIAN, 1998) automatic calibration algorithm was employed jointly with the MGB-SED (BUARQUE, 2015) model to carry out 10 experiments, which resulted in 37 automatic calibrations and 111 validation tests.

Table 1. Summary of the application of sediment models that uses automatic calibration. This table does not exhaust all published studies on this subject. The last study in this list refers to the current study.

Study	Model	Calibration Methods	Basin (Country)	Area (km²)	Years/ Data for calibration	Years/ validation data	Nº of station	Temporal Scale
Santos et al. (2003)	WESP	SCE-UA	Sumé (Brazil)	0.0048	45 / Sed.	-	4	Events
Muleta and Nicklow (2005)	SWAT	Unnamed	Big Creek (US)	133	2 / Sed.	1/ Sed.	2	Daily
Van Rompaey et al. (2005)	WaTEM/ SEDEM	-	40 basins (Italy)	11-697	30-50 / Sed.	unclear	40	Yearly
Bekele and Nicklow (2007)	SWAT	NSGA-II	Big Creek (US)	133	2 / Sed.	2/Sed.	2	Daily
Rostamian et al. (2008)	SWAT	SUFI-2	Beheshtabad and Vanak (Iran)	3860 and 3198	6.75 and 10.66 / Sed.	2.25 and 5.33 / Sed.	4 and 4	Daily
Yin et al. (2009)	APEX	Unnamed (Wang et al., 2006 procedure)	Three Plots in Middle Huaihe (China)	0.0006, 0.0010 and 0.0014	7, 10 and 9 / Sed.	6, 8 and 6 / Sed.	3	Events[1]
Santos et al. (2010)	WESP	RPS	Sumé (Brazil)	0.0048	38 / Sed.	-	4	Events[1]
Betrie et al. (2011)	SWAT	ParaSol	Blue Nile (Ethiopia / Sudan)	-	7 / Sed.	7 / Sed.	1	Daily
Bezak et al. (2015)	WATEM/ SEDEM	PEST	Kuslovec, Soca, Idrijca, Savinka and Sava (Slovenia)	0.7, 435, 443, 1842 and 1951	11 / Sed.	-	5	Yearly
Singh et al. (2014)	SWAT and RBNN	SUFI-2	Nagwa (India)	92	14 / Sed.	3 / Sed.	1	Monthly
Yesuf et al. (2015)	SWAT	SUFI-2	Maybar (Ethiopia)	0.113	7 / Sed.	6 / Sed.	1	Monthly
Ayele et al. (2017)	SWAT	SUFI-2, GLUE, ParaSol, and PSO	Koga (Ethiopia)	287	13 / Sed.	6 / Sed.	1	Monthly
Stewart et al. (2017)	MUSLE, DHSVM and MRC	Borg	Clear Creek (US)	1024	50 / Sed.	-	1	Daily
Worku, Khare and Tripathi (2017)	SWAT	SUFI-2	Beressa (Ethiopia)	213	20 / Sed.	15 / Sed.	1	Monthly
Yen et al. (2017)	SWAT	IPEAT	Arroyo Colorado (US)	1692	1 / Sed.	1 / Sed.	1	Monthly
Fagundes et al. (the present study)	MGB-SED	MOCOM-UA	Doce (Brazil)	86715	14/ Sed., Turbidity, TSS² and SSR³	14/ Sed, Turbidity, TSS² and SSR³	24, 63, 63 and 21	Daily

[1]Some studies have used rainfall events with variable time instead of a day or a month; ²Total Suspended Soils; ³Surface spectral reflectance.

DATA AND METHODS

Study area

The study area is the Doce River basin (Figure 1a of the supplementary material), considered by Lima et al. (2005), among the great Brazilian basins, that one that has the largest SSC average (386.25 mg/L). It is a very emblematic basin, since it is where, on November 5th, 2015, the infamous Mariana Dam Disaster occurred, afflicting a great part of the Doce River, and leading to rampant environmental impacts (ANA, 2016). Aside from these reasons, the basin was selected due to the presence of a relatively large number of stations having observed data (Figure 1a of the supplementary material).

It has an area of approximately 86,715 km² (PIRH, 2010) and is located between the states of Minas Gerais and Espírito Santo. The basin has a strongly seasonal rainfall pattern (PINTO; LIMA; ZANETTI, 2015) presenting a dry season that varies from April to September, and a rainy season varying from October to March (Figure 1b of the supplementary material). The strong and concentrated rainfall contribute to the intensity of erosive processes in the basin, causing siltation issues in the reservoirs (FAN et al., 2015b). The predominant types of soil within the region are Red-Yellow Latosols and Red Argisols. There are also other types of Latosols and Argisols, Litholic Neosols, Gleysols and Cambisols (PIRH, 2010).

Fagundes et al. (2017) showed that the basin sediment yield varies from around 10 t/ano.km² to close to 14,680 t/ano.km². The authors also demonstrated that sediment yield is directly linked to the increase in slope; also that regions south of the Doce River tend to hold the highest sediment yield values. Furthermore, Fagundes et al. (2017) observed that sediment discharge increases along with the drainage area, reaching values higher than 7,000,000 t/day in the Doce River. Tributaries, transporting the largest sediment load, are the Piracicaba, Santo Antônio, Suaçuí Grande and the Manhuaçu Rivers.
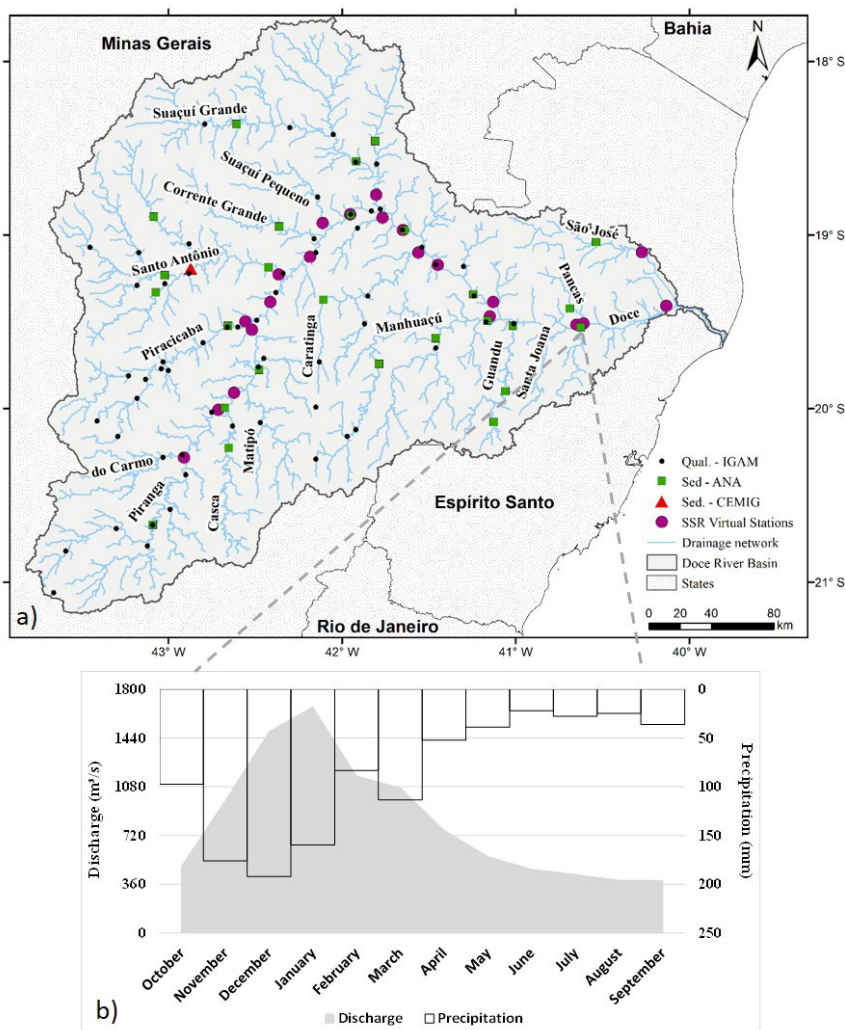

Figure 1. (a) Doce river basin, main rivers, and locations of ANA and CEMIG suspended sediment concentration monitoring station, IGAM water quality stations, and virtual surface reflectance stations; (b) Long-term monthly average (1970-2010) hyetograph and hydrograph at stations 1940006 and 56994599, respectively, located in Colatina - ES.

Datasets

Suspended sediment concentration

We obtained information stemmed from 24 SSC monitoring stations (Figure 1) from the National Water Agency (ANA), made available through the Hydrological Information System (HidroWeb), possessing around four annual measurements between 1997 and 2010 (surrogate data was also acquired for this period). SSC data was also obtained from the Fazenda Ouro Fino station (Figure 1), provided by the Minas Gerais Energy Company (CEMIG), which holds around one daily measurement over the rainy season, and from four to ten measurements for dry-season months.

Turbidity and total suspended solids

Turbidity and total suspended solids (TSS) data was obtained from 63 water quality monitoring stations (Figure 1) of the Minas Gerais Water Management Institute (IGAM), taking around four annual measurements. This data was used as a proxy of SSC, despite them considering other substances suspended in water (ASTM, 2003) besides the inorganic soil fractions (silt, clay and sand), which is the SSC case. This was performed since various studies (e.g. GLYSSON; GRAY; CONGE, 2000; WILLIAMSON; CRAWFORD, 2011; PAVANELLI; BIGI, 2005; MINELLA et al.,

2008; SARI; CASTRO; PEDROLLO, 2017) demonstrated that there is a substantial correlation between SSC and these water quality data.

Spectral surface reflectance

Studies indicate that it is possible to use the visible (~0.40 μm to 0.70 μm) and infrared (~0.70 μm to 1.30 μm) electromagnetic spectrum to evaluate water components through remote sensing (LODHI et al., 1998; MUNDAY JUNIOR; ALFÖLDI, 1979). The red band is one of the most used in SSC estimation, for it is where the peak of reflectance occurs in water-sediment mixtures (LODHI et al., 1998). On the other hand, reflectance saturation may occur for high SSC, causing reflectance to not increase proportionally to SSC (LODHI et al., 1998). Among the advantages of using SSR to monitor SS are the low financial cost in acquiring images and the possibility to obtain information with wide spatial coverage and with high temporal frequency (WANG et al., 2009; ESPINOZA VILLAR et al., 2012). Among the disadvantages are the limited use of SSR in rivers that are too narrow, once the water-sediment mixtures reflectance value may be influenced by the presence of river banks and/or sand bars, both in rainy and dry seasons (e.g. MARTINS et al., 2017).

21 virtual stations across the Doce River basin were created using images from the Landsat 5/ TM satellite (Figure 2), where
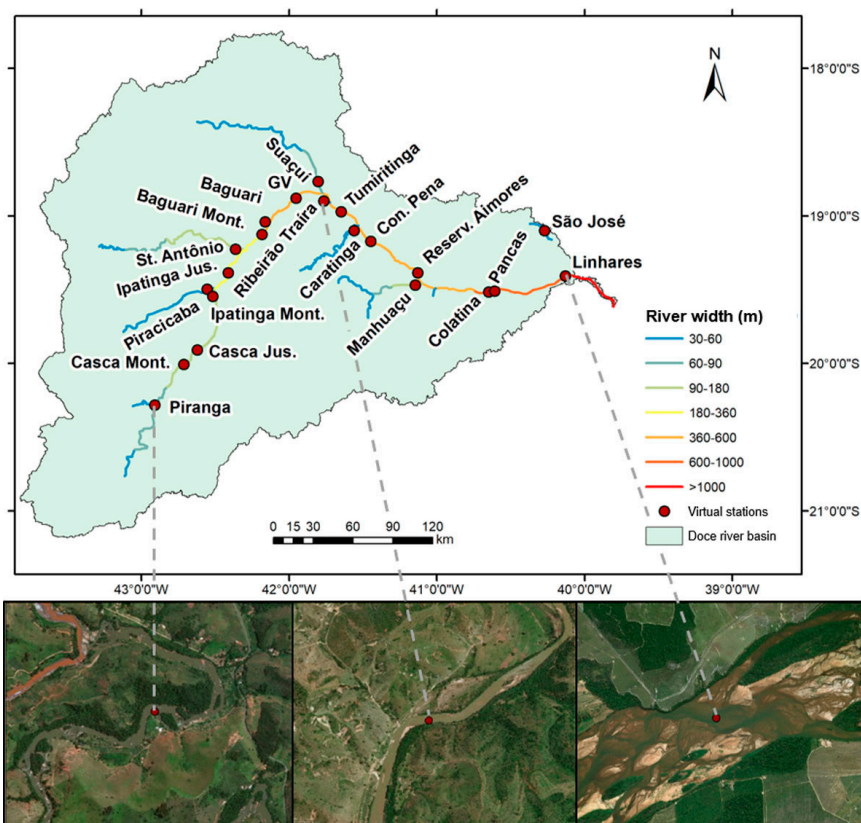

Figure 2. Potential locations for red band surface reflectance extraction in the Doce River basin (0.64 μm-0.67 μm) and virtual stations created from Landsat 5/ TM images. Satellite images in the natural composition show details of reflectance extraction places for stations Piranga, Suaçuí and Linhares.

SSR information was extracted in the red band. The Landsat 5/ TM satellite was chosen because it presents a long temporal series of the past, 30m spatial resolution and also due to institutions that already provide that product with atmospheric corrections. In the present study, images were acquired at no charge from the United States Geological Survey - USGS (2018a) with atmospheric correction (USGS, 2018b). To encompass the entire basin, images from four scenes with the following orbit/point were used: 216/073, 216/074, 217/073 and 217/074. An average of 13 images per year were used for each scene, due to images with high cloud cover (>80%) not being used. SSR data extraction was performed through the same approach proposed by Fagundes, Paiva and Fan (2017), which seeks to obtain information on pixels free from cloud and shadow interference.

A procedure that could have been adopted to work with the remote sensing data would be their transformation in SSC through empirical relationships, as performed by Martinez et al. (2009), Espinoza Villar et al. (2012), Zhang et al. (2014) and others. In the current study, however, a simpler possibility was tested, one that allows for a broader use of information, which would be the direct use of reflectance in comparing to the sediment model results, following the procedure presented in the "Experiments" section.

The MGB-SED Model

The MGB-SED (BUARQUE, 2015) model is coupled to the MGB large-scale hydrological model (COLLISCHONN et al., 2007), which is a distributed and conceptual model, with daily time step, unit catchments discretization, and that uses the Hydrologic Response Units (HRU) approach. MGB-SED was developed to represent the erosion and sediment transport processes in hill slopes, as well as to depict channel sediment transport with possible interactions with floodplains. The sediment yield at each unit catchments is estimated through MUSLE (Equation 1) (WILLIAMS, 1975), considering a *LS* two-dimensional topographic factor (BUARQUE, 2015) extracted from the Digital Elevation Model (DEM), using surface runoff volumes calculated by MGB as an input. Fine sediments (silt and clay) are routed along the river as suspension loads by the diffusion-advection equation and don't settle into the channel.

$$Sed = \alpha \cdot \left(Q_{sur} \cdot q_{peak} \cdot A \right)^{\beta} \cdot K \cdot C \cdot P \cdot LS \qquad (1)$$

where *Sed* [t/day] is the sediment load resulting from soil erosion, Q_{sup} [mm/ha] is the surface runoff volume, q_{pico} [m^3/s] is the peak flow rate, A is the superficial area, α and β are the adjustment coefficients (which are calibrated afterwards), whose values originally estimated by Williams (1975) were 11.8 and 0.56, Rspectively, K [0.013.t.m^2.h./m^3.t.cm] is the soil erodibility factor, C [-] is the cover and management factor, P [-] is the conservation practice factor and LS [-] is the topographic factor.

A model with the configurations defined by Fagundes et al. (2017) was employed in this study, which they used in the Doce River basin and obtained good results in the calibration process. A brief description of these settings follows.

The Doce River basin was discretized into 1173 unit catchments (Figure 1c of the supplementary material) and the HRU were acquired from the South America HRU map (FAN et al., 2015a). We use 217 rainfall and 59 ANA flow stations, along with 14 meteorological stations from MGB internal database (FAN; COLLISCHONN, 2014). The employed channel flow routing method was the Muskingum-Cunge, which has shown satisfying results in basins with no significant effects of backwater and floodplain storage (e.g. ALLASIA et al., 2015; COLLISCHONN et al., 2007; TUCCI; BRAVO; COLLISCHONN, 2009; GETIRANA et al., 2010; NÓBREGA et al., 2011; FAN et al., 2016).

The q_{peak} was calculated from the daily uniform surface runoff volume (BUARQUE, 2015). The *LS* factor is the combination of the slope-length L and slope-steepness S factors. This factor was calculated using Buarque (2015) methodology, who developed a computational routine that computes the *LS* factor two-dimensionally, making use of Desmet and Govers (1996) approach to determine the L factor, and the Wischmeier and Smith (1978) equation to determine S factor.

Value of P factor was adopted equal to 1 for two reasons: i) conservation practices have greater impact in small watersheds. With the increase of the watershed, its impacts can be despised or may not cause significant difference in the estimates performed by the model; and ii), due to the hardship of obtaining the P values for large basins. Factor K was estimated following the equation proposed by Williams (1995), which uses soil texture data, obtained from the Food and Agriculture Organization of the United Nations (FAO, 1971), displayed on Table 2. Factor C values for each HRU are also indicated within that table, obtained from the literature (see FAGUNDES et al., 2017).

Table 2. Parameters used for sediment yield estimation through MUSLE.

HRU	SOIL	SAND (%)	SILT (%)	CLAY (%)	ORGC (%)	C
Shallow soil forest	Cambisols and Litosols	65.55	15.55	18.90	0.87	0.04
Deep soil forest	Argisols and Latosols	44.50	16.75	38.75	1.84	0.04
Shallow soil agriculture	Cambisols and Litosols	65.55	15.55	18.90	0.87	0.164
Deep soil agriculture	Argisols and Latosols	44.50	16.75	38.75	1.84	0.164
Shallow soil field	Cambisols and Litosols	65.55	15.55	18.90	0.87	0.05
Deep soil field	Argisols and Latosols	44.50	16.75	38.75	1.84	0.05
Wetlands	Argisols	53.30	17.20	29.50	1.74	0.000
Semi-impervious area	Argisols and Latosols	44.50	16.75	38.75	1.84	0.001
Water	-	0	0	0	0	0

Source: Fagundes et al. (2017).

Procedures for automatic calibration

According to Moriasi et al. (2007), calibration is the process of estimating the model parameters through comparisons between a model estimation and an observed data set, both in similar conditions. Validation is used here as defined by Refsgaard (1997): as the process that demonstrates that a specific model is capable of performing "sufficiently accurate" simulations for a location. The term "sufficiently accurate" being subjective and related to goals to be achieved.

The MGB-SED model was calibrated using the MOCOM-UA multi-objective automatic calibration algorithm (YAPO; GUPTA; SOROOSHIAN, 1998), which has already been implemented in the MGB model (FAN; COLLISCHONN, 2014). Some modification was necessary to calibrate parameters related to sediment load estimation. The adjustment coefficients α and β present in MUSLE (Equation 1) were adopted as calibration parameters. These parameters have been modified in several studies, as shown by Sadeghi et al. (2014) in their review paper about MUSLE applications around the world, in which about 30% of the papers have carried out alterations of these parameters. A surface runoff delay parameter (*TKS*) from the MGB-SED model was also adopted to calibration procedures. Sediment volumes generated at each HRU are virtually stored in a linear reservoir, which is a structure that transports sediments from the unit catchments to the river channel. *TKS* parameter is associated to the linear reservoir (COLLISCHONN et al., 2007), and determines the period in which sediments reach the channel. *TKS* was computed for each unit catchment and is directly related to their time of concentration. After setting *TKS* value, changes were considered at the sub-basin level (or to the whole basin, if that were the case); that is, every *TKS* value was amplified or reduced at the same rate, but each unit catchment could have a single *TKS* value. A sensitivity analysis was also performed for each calibration parameter.

The MOCOM-UA algorithm uses genetic algorithm techniques and has Nelder and Mead simplex algorithm (SOROOSHIAN; GUPTA, 1995) in its structure. To make use of the MOCOM-UA it is necessary to define the number of parameters (N) to undergo calibration; the search space limits that each parameter may take; the number of objective functions (NF) to evaluate the model; and the parameter set number (NS) or points (defined randomly) within the region determined by the space limits. Each point is provided by the N parameter values and, for each point, the NF objective functions are assessed, providing a result matrix F(NS, NF) (COLLISCHONN; TUCCI, 2003).

To perform multi-objective automatic calibration it is necessary to define, beyond calibrated parameters, which objective functions will be used to evaluate the desired quality adjustment. Moreover, the MOCOM-UA algorithm seeks to optimize these functions simultaneously. The main characteristic of a multi-objective optimization problem is that the solution, generally, will not be a single one (COLLISCHONN; TUCCI, 2003). The value that presented the best objective function average for a given data set was always the selected one for the calibration in this study. The calibrated parameter values adopted for each experiment may be found in the supplementary material. Further information regarding the automatic calibration method used in this study, as well as other information about the subject can be found in Collischonn and Tucci (2003).

Experiments

In order to investigate how remote sensing and water quality data may be used in calibrating and validating sediment models, as well as aiding towards potential enhancements, several experiments were conducted and compared to a reference simulation in which the model was not calibrated. The reference simulation was performed considering the values α=11.8 and β=0.56 (WILLIAMS, 1975), *TKS* without variation and 17 sub-basins. 10 experiments were performed (Table 3), all having the same calibration and validation period: 1997-2010. In each experiment,

Table 3. Experiments for calibrating and validating the MGB-SED hydrosedimentological model with different data sources.

Experiment	Nº of sub-basins	Objective functions	Calibration	Observations
E1	1	Rtp, Rsp, Rgl	SSC, SSR, Turbidity, TSS	-
E2	5	Rtp, Rsp, Rgl	SSC, SSR, Turbidity, TSS	-
E3	17	Rtp, Rsp, Rgl	SSC, SSR, Turbidity, TSS	-
E4	17	Rtp, Rsp, Rgl	SSClog, SSR, Turbidity, TSS	SSC transformation into SSClog
E5	17	Rtp, Rsp, Rgl	QSS, SSR, Turbidity , TSS	Use of observed and calculated QSS instead of SSC
E6	17	Rtp, Rsp, Rgl	SSC, SSR, Turbidity , TSS	Only observed and calculated SSC data > 50 mg/L was used
E7	17	Rtp, Rsp, Rgl	SSC, SSR, Turbidity , TSS	Use of background concentration
E8*	17	Rtp, Rsp, ENS	SSC, SSR, Turbidity , TSS	α search interval between 10.0 and 13.0, β between 4.0 and 7.0, *TKS* between 0.5 and 1.5, Imaxgen equal to 100, and SSCbg
E9*	17	Rtp, Rsp, Rgl	SSC, SSR, Turbidity , TSS	α search interval between 0.00001 and 3.0, β between 0.00001 and 0.5, *TKS* between 0.5 and 1.5, and SSCbg
E10	17	ENS, KGE, Rtp	SSC	Calibration for only 1 station

In the table, SSC is the suspended sediment concentration; SSR is spectral surface reflectance in red band; TSS are total suspended solids; Rtp is the temporal correlation coefficient; Rsp is the spatial correlation coefficient; Rgl is the global correlation coefficient; KGE is the Kling-Gupta coefficient; ENS is the Nash-Sutcliffe efficiency coefficient; Imaxgen is the maximum value for algorithm iteration; QSS is the suspended solid discharge; SSCbg is the SSC background concentration that always remained in the river. All experiments made use of all datasets to validation; *For these experiments, SSC stations 56800000, 56846000 and 5697600, Turbidity stations RD091 and RD098 and TSS RD098 and RD099 stations were not considered, and a second reference simulation was performed (without calibration).

generally, one type of data (e.g. SSC measured in situ) was used for the model automatic calibration, while the others (e.g. SSR, turbidity and TSS) were used for validation, which resulted in 4 calibrations in the case of experiment E1, for example. Other elements that influenced the type of experiment to be performed were the number of sub-basins (1, 5, and 17), and the objective functions (always three for each experiment, which may be distinct). Spatial discretization of the basin are illustrated in Figure 1 of the supplementary material.

The objective functions used in the automatic calibration were the Nash-Sutcliffe efficiency coefficient (ENS) (NASH; SUTCLIFFE, 1970), Kling-Gupta efficiency coefficient (KGE) (GUPTA et al., 2009), Pearson correlation coefficient (Rtp) (ELSEL; HIRSCH, 1992), and its variations, named spatial correlation coefficient (Rsp) and global correlation coefficient (Rgl), explained in the text below. The MOCOM-UA algorithm aims to optimize each of the objective functions, to that end, a single value derived from these functions is necessary. For ENS and KGE, the objective function value (OFV) was calculated according to Equation 2.

$$OFV = \sum_{i}^{n} \left(1 - \text{"coefficient value of station } i\text{"} \right) \qquad (2)$$

As Rtp results in a single value for each station, an average Rtp value from all of them subtracted from the unit was used (Equation 3). In order to calculate Rsp two new data series were built: one composed by the long-term average of observed values for each station, and the other by the long-term average of the simulated values to the corresponding station. It was also built two data series to estimate Rgl: one with all observed values from all stations, and the other with their respective simulated values. After we have defined the series, the Pearson was computed for both Rsp and Rgl. OFV for Rsp and Rgl is calculated in the same way as Equation 3, just changing the variable $\overline{Rtp}$ to Rsp and Rgl.

$$OFV = 1 - \overline{Rtp} \qquad (3)$$

Table 3 summarizes the experiments and illustrates their specific characteristics. For most experiments, a search space for parameter α was set between 2.0 and 25.0, for β between 0.2 and 1.7,

and *TKS* between 0.1 and 3.0, with a maximum number of algorithm iteration (Imaxgen) at 60, and 50 parameter sets (NS). Since parameters α and β are not physically based, and *TKS* can have broad variations due to the several real conditions that may retain sediments over the basins, these ranges could be different. However, they were defined through the sensitivity analysis of these calibrated parameters.

Experiments E1, E2 and E3 were performed by varying the number of sub-basins (calibration elements) at 1, 5 and 17, Respectively, to investigate whether the model better represented sediment processes when the calibration parameter set was more heterogeneous. Other experiments were carried out to investigate whether highest correlation values would be achieved when correlations between observed SSC derived data and simulated data from MGB-SED were calculated. These were the case of the experiments E4, in which SSC data was converted into the logarithm of SSC (logSSC); E5, in which SSC was converted into QSS; E6, in which only SSC values higher than 50 mg/L (a value hardly exceeded in measurements taken during the dry season in the Doce River basin) were used; and E7, which a background concentration (SSCbg) was employed to attempt to enhance the representation of SSC values. SSCbg was computed as the average of SSC values measured in the dry season, for each sediment station. Aiming to verify the influence of certain automatic calibration algorithm parameters, experiments E8 and E9 were conducted. In the experiment E10, the model was calibrated for the Fazenda Ouro Fino - CEMIG, which is the station with the highest number of SSC observed data. For this latter, the found calibrated parameter values were applied all over the basin.

RESULTS

Sensitivity analysis

MUSLE parameters α and β affect the amount of sediments generated at each HRU, while the affect the time in which these sediments arrive at the drainage network. Figure 3 shows that sediment graphs are amplified or reduced proportionally to the
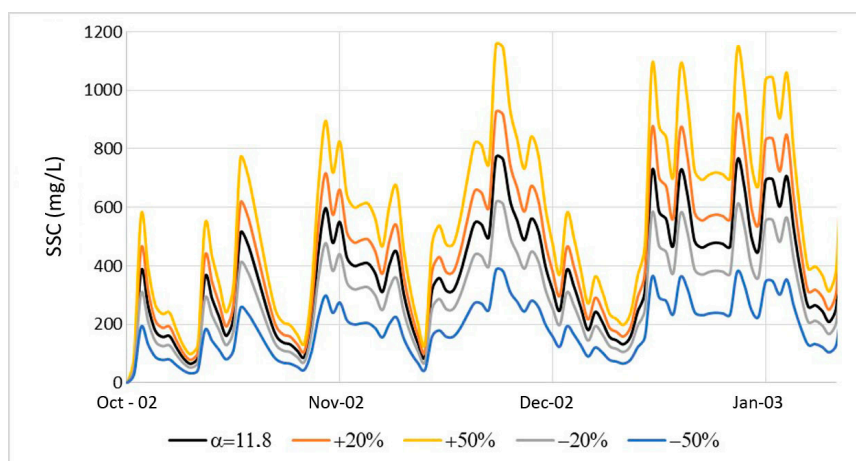

Figure 3. Sensitivity analysis of suspended sediment concentration simulated by MGB-SED for α parameter changes in Piranga-MG.

parameter value variation α, meaning a 20% increase in the α value will cause a 20% increase in the SSC value. Parameter β, however, amplifies the sediment graphs and intensifies their peaks and valleys at the rate its value decreases, which is evidenced in the blue line (-50%) on Figure 4. Changes to β are not proportional, a 20% increase in the parameters value caused, on average, a reduction of 66% in the SSC value. This happens due to the β parameter being the exponent of a value that is always less than 1.

Figure 5 exhibits the MGB-SED results in the face of changes to the   parameter. It is observed that the smaller the   value, the more intense are the peaks and valleys, as shown by the sediment graph in blue (-50%). A 50% decrease in   value could cause an increase of up to 7,300% in the SSC value. Furthermore, a change to the   value causes a temporal variation in the sediment graph, anticipating the SSC peak. Comparing the sediment graph in yellow (+50%) to the sediment graph in blue inside the marked rectangle in Figure 5, a near 2 days discrepancy is noted in the SSC peak and its reduction from 953 mg/L to 660 mg/L.

Deviations in calibrated parameters values may result in large differences in the values estimated by the MGB-SED model, especially in the amplification of extreme values. For an appropriate representation it is important to establish a search space during the automatic calibration process that results in simulated values that are consistent with observed values.

Experiment analysis

In this section the results of the experiments are briefly outlined, they support the subsequent discussion. To aid in the comprehension of the results presented in the form of tables, the average difference (AD) and the average absolute difference (AAD) were calculated. AD was calculated as the average between the values presented in the tables, considering whether they are positive or negative, to verify how much the results improved or worsened. AAD was calculated similarly, but without considering the sign of the values, in order to indicate the difference magnitude of the results.
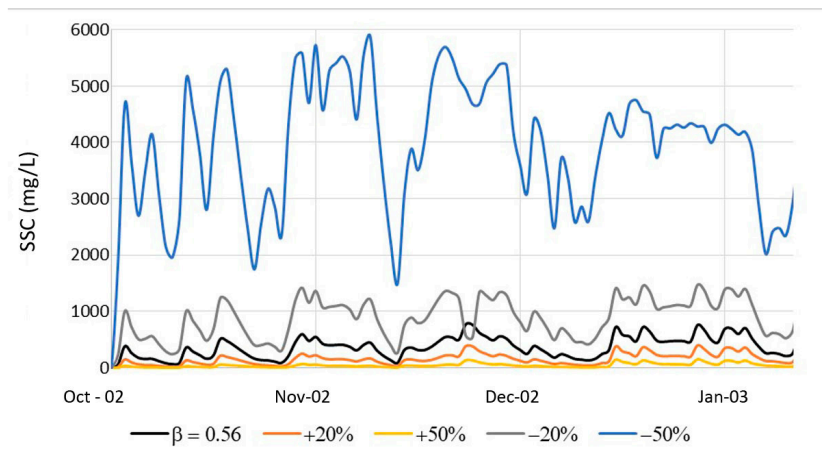

Figure 4. Sensitivity analysis of suspended sediment concentration simulated by MGB-SED for β parameter changes in Piranga-MG.
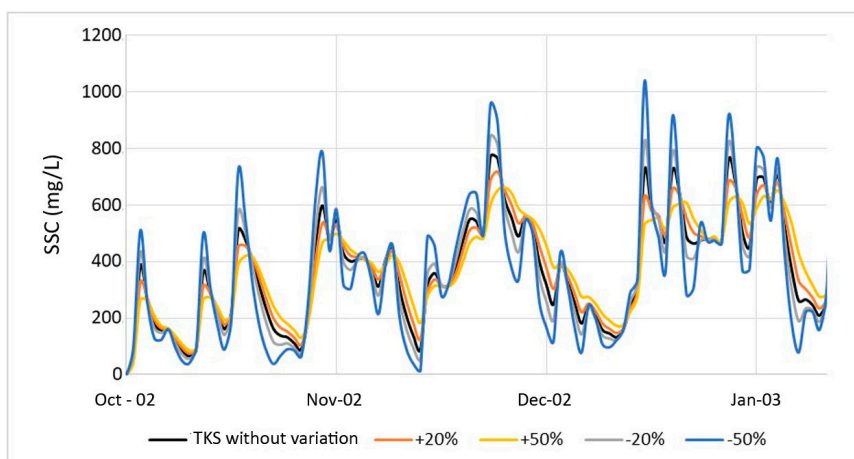

Figure 5. Sensitivity analysis of suspended sediment concentration simulated by MGB-SED for *TKS* parameter changes in Piranga-MG.

Sub-basin numbers deviation

Table 4 exhibits the comparison between experiments that had the number of sub-basin changed. Both in that table as in the others that follow that template: values represent the absolute increase (green) or decrease (red) in relation to the values in the reference simulation (without calibration); the main diagonal represents the metric values related to calibration; the values on the other cells represent the metric values regarding validation.

Table 4 results show that in the calibration period, metrics are generally better, while in the validation period they are worse, which is common within the context modelling (e.g. BUSSI et al., 2014; YESUF et al., 2015; AYELE et al., 2017; WORKU; KHARE; TRIPATHI, 2017). Nevertheless, the metrics worsening was not significant, proving that all data assisted in the model validation process. It should be noted that the E1 experiment (1 sub-basin) is the one that have the smallest differences, both in the calibration (AAD = 0.02) as in validation (AAD = 0.02) period. With the increase of sub-basin numbers from 1 to 5, AD increased from 0.01 to 0.06 in the calibration step. In increasing from 5 to 17 sub-basins, the results exhibit little difference, with some values remaining the same. Experiment E3 (17 sub-basins) shows that reflectance was the dataset in which the correlation average had the most increase (0.12), even when using turbidity data (0.06) and TSS (0.06) to calibrate MGB-SED.

Comparison with SSC derived data

The results of experiments E5 (QSS) and E6 (SSC values higher than 50 mg/L) showed low or even negative correlation values. For these experiments, results tables are not be presented. Although the MGB-SED model may have underestimated observed values in the dry season during the current application, in trying to calibrate it only taking into consideration SSC values > 50 mg/L, the results do not showed enhancements. In establishing a SSC threshold, the amount of observed data available for comparison decreased, and the sediment temporal variability was worse.

Table 5 presents the results of experiments E4 (SSClog) and E7 (SSCbg). Experiment E4 highlights the improvement of mean values of correlations between simulated and observed SSClog, both in calibration (+0.14) as in validation (+0.25). On the other hand, for turbidity and TSS data, both calibration (AD=-0.19) as validation (AD=-0.19) presented worse correlation values. When a background SSC was included, in calibration AD increased by 0.10, and in validation it decreased by -0.07 It is emphasized that the best model performance, during the calibration step using SSC data, was in experiment E7. In a certain way, this fact was expected, once the observed SSC values themselves were used to calculate the SSCbg.

Changes in automatic calibration parameters

Table 6 presents the results for experiments E8 (smaller search space and greater Imaxgen) and E9 (small α and β values). The more restricted the search space, smaller are the possibilities of combinations being able to generate an optimal result. This procedure could make the search algorithm found a local maximum instead of a global maximum. It is observed that in experiment E8, the calibration performed with SSR data resulted in higher metric values for SSC results in the validation. In experiment E9, it is noted that the metrics were improved only for SSC and SSR data during the calibration. For turbidity and TSS data, automatic calibration did not find a better parameter set than those from the reference simulation, thus the results did not show changes.

Table 4. Result comparisons for experiments E1, E2 and E2, where sub-basins 1, 5 and 17 were respectively used.

| | E1 (1 SUB-BASIN) | | | | E2 (5 SUB-BASINS) | | | | E3 (17 SUB-BASINS) | | | |
| | Validation | | | | Validation | | | | Validation | | | |
Calibration	SSC	SSR	Turb.	TSS	SSC	SSR	Turb.	TSS	SSC	SSR	Turb.	TSS
SSC	**0.02**	-0.07	-0.03	-0.05	**0.05**	-0.03	-0.01	-0.03	**0.05**	-0.02	-0.02	-0.04
SSR	0.00	**-0.01**	0.01	0.00	-0.08	**0.12**	-0.03	-0.01	-0.08	**0.12**	-0.05	-0.04
Turb.	0.00	-0.04	**0.02**	0.01	0.00	0.04	**0.03**	0.02	-0.02	0.06	**0.02**	0.03
TSS	0.01	-0.02	0.02	**0.01**	-0.06	-0.03	0.03	**0.02**	-0.02	0.06	0.02	**0.03**

The values within the cells represent the increase (green) or decrease (red) in relation to the average of the three correlations (temporal, spatial and global) when compared to the reference simulation values (without calibrating): SSC – 0.50; SSR – 0.63; Turb. – 0.63; TSS – 0.65. The results of the main diagonal (in bold) refer to the calibration process while the others refer to the validation process, both performed for 1997-2010 period.

Table 5. Result comparisons for results E4 (SSClog) and E7 (SSCbg), where different SSC derived data was employed.

| | E4 (SSC LOGARITHM) | | | | E7 (SSCBG) | | | |
| | Validation | | | | Validation | | | |
Calibration	SSC	SSR	Turb.	TSS	SSC	SSR	Turb.	TSS
SSC	**0.14**	-0.11	-0.01	-0.08	**0.17**	-0.10	-0.20	-0.26
SSR	0.23	**0.09**	-0.13	-0.22	0.02	**0.10**	-0.10	-0.08
Turb.	0.29	-0.15	**-0.07**	-0.12	0.00	-0.12	**0.05**	0.06
TSS	0.23	-0.15	-0.07	**-0.12**	-0.02	-0.12	0.05	**0.07**

The values within the cells represent the increase (green) or decrease (red) in relation to the average of the three correlations (temporal, spatial and global) when compared to the reference simulation values (without calibrating): SSC – 0.50; SSR – 0.63; Turb. – 0.63; TSS – 0.65. The results of the main diagonal (in bold) refer to the calibration process while the others refer to the validation process, both performed for 1997-2010 period.

These results show that the parameter sets that present values closest to those found by Williams (1975), α, especially, result in better model performances.

Results from experiment 8 are detailed on Table 7. The main improvements occur during calibration, for Rsp values (AD=0.24). Considering only SSC, Resp values increase from 0.36 (in reference simulation) to 0.79 after the model has been calibrated. On the other hand, Rtp values, on average, had slight variations (AAD=0.01). Improvements in Rsp values indicates that observed and simulated values became closer for each station after automatic calibration procedure.

Fazenda Ouro Fino station

During experiment E10, MGB-SED was calibrated using ENS, KGE and Rtp statistics for the Fazenda Ouro Fino station (area ~ 6.438 km²). Results showed that Rtp after calibration remained equal to 0.64; KGE increased from -0.19 to 0.52; and the experiment most significant result is the enhancement in the ENS coefficient, which increased from -0.44 to 0.44. Figure 6 shows SSC values observed and simulated at the Fazenda Ouro Fino station, and it is possible to note that simulated values after calibration were smaller. That is due to the characteristics of the employed metrics (e.g. ENS) combined with the optimization

Table 6. Result comparison for experiments E8 (smaller search space and larger Imaxgen) and E9 (small α and β values).

	E8 (SMALLER SEARCH SPACE AND LARGER IMAXGEN)				E9 (SMALLER VALUES FOR α AND(β))			
	Validation				Validation			
Calibration	SSC	SSR	Turb.	TSS	SSC	SSR	Turb.	TSS
SSC	**0.16**	0.00	-0.07	-0.10	**0.06**	-0.08	-0.31	-0.35
SSR	0.03	**0.11**	-0.03	-0.03	-0.07	**0.08**	-0.09	-0.07
Turb.	-0.20	-0.16	**0.01**	0.02	0.00	0.00	**0.00**	0.00
TSS	-0.19	0.03	-0.03	**0.08**	0.00	0.00	0.00	**0.00**

The values within the cells represent the increase (green) or decrease (red) in relation to the average of the three correlations (temporal, spatial and global) when compared to the reference simulation values (without calibrating): SSC - 0.51; SSR – 0.63; Turb. – 0.65; TSS – 0.65. The results of the main diagonal (in bold) refer to the calibration process while the others refer to the validation process, both performed for 1997-2010 period.

Table 7. Detailed values of metrics found through experiment E8 (search space smaller and Imaxgen larger).

	Rsp				Rtp				Rgl			
	Validation				Validation				Validation			
Calibration	SSC	SSR	Turb.	TSS	SSC	SSR	Turb.	TSS	SSC	SSR	Turb.	TSS
SSC	**0.43**	0.01	-0.18	-0.29	**0.02**	0.01	-0.01	-0.02	**0.04**	-0.02	-0.02	0.01
SSR	0.10	**0.30**	-0.06	-0.07	0.01	**0.01**	0.00	0.00	0.00	**0.01**	-0.01	-0.02
Turb.	-0.22	-0.38	**0.02**	0.04	-0.11	-0.01	**-0.01**	0.01	-0.28	-0.09	**0.01**	0.01
TSS	-0.20	0.14	-0.10	**0.21**	-0.12	-0.01	-0.01	**0.01**	-0.23	-0.03	0.00	**0.03**

The values within the cells represent the increase (green) or decrease (red) in relation to the average of the three correlations (temporal-Rtp, spatial-Rsp and global-Rgl) when compared to the reference simulation values (without calibrating): SSC - 0.51; SSR– 0.63; Turb. – 0.65; TSS – 0.65. The results of the main diagonal (in bold) refer to the calibration process while the others refer to the validation process, both performed for 1997-2010 period.
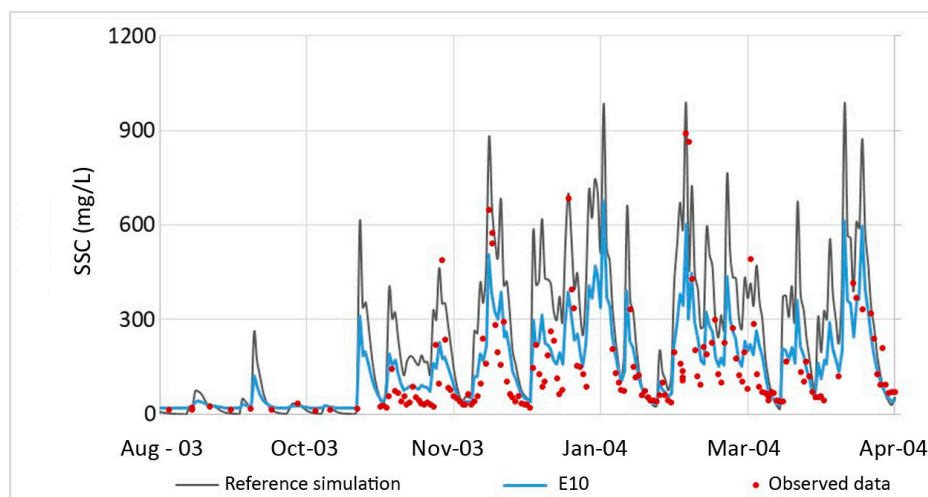
Figure 6. SSC values calculated and observed at Fazenda Ouro Fino (CEMIG) station. Calibrated SSC values were calculated from experiment E10.

algorithm, which jointly aim to minimize absolute errors between observed and simulated data.

Results from experiment E10 are important in showing that the metrics used, and calibration for a single station significantly improved the MGB-SED performance. Furthermore, results indicate that the improvements that can be reached also depend on the amount of stations and, especially, of available data at each one of them. For instance, Fazenda Ouro Fino station is the one with the largest number of available information, while a large part of the stations used in the other experiments just have 4 yearly observations.

Summary of analyzes

When statistic metric values were larger during calibration for a specific dataset, in general, metric values were smaller for the other datasets during validation. This point out that, although all types of data present information related to SS, there are divergences in the methodology of estimating this data and in representing the spatio-temporal dynamic of sediments within the basin. However, analyzes carried out from the experiments allowed for a few important considerations, outlined as follows:

- In increasing the number of sub-basins, results tend to improve due to the better representation of the basins heterogeneity;

- The calibration performed for a station that show a long and dense data time series, using metrics that represent the correlation, bias and amplitude of variation, tends to provide better estimates of SSC simulated;

- The replacement of SSC values by their logarithms increased metric values both in calibration and in validation in the case of SSC data; while, generally, decreased the metric values for SSR, turbidity and TSS during validation, as well as in turbidity and TSS calibration;

- Including a background concentration increased the metric values during calibration for all datasets, especially for SSC data;

- The reduction of search space around the standard calibrated parameter values (α=11.8 β =0.56 and *TKS* without changes), with a large number of iterations resulted in higher average correlation values than when that search space was bigger.

DISCUSSIONS

Observational data for calibration

Several limitations and uncertainties were present in the calibration and validation processes using the MGB-SED model, and that influenced the results obtained. Firstly, taking observed data into consideration, we realize that there are uncertainties associated with them and their acquisition way (OP DE HIPT et al., 2017), and despite all of them being related to suspended sediments, the used approaches and methods are different. Methods employed

for SSC acquisition usually considered only inorganic sediments in water suspension (BOITEN, 2008). Turbidity may be influenced by suspended and/or dissolved organic matter in the water (ASTM, 2003). Reflectance, however, considers every water suspended matter that interacts with solar radiation (JENSEN, 2009).

According to Morris and Fan (1998), sampling and analysis programs are usually inadequate in determining long-term sediment loads. That is because SS measurements, used to validate the models, are generally scarce for periods of high stream flows and catastrophic events. One of the techniques used in those situations is the extrapolation of curve fitting to a period beyond that of observed data. This extrapolation might be a possible source of errors and uncertainties (MORRIS; FAN, 1998). Figure 6 illustrates that the application of the MGB-SED model in the Doce River basin as it was done, could not represent the great peaks of SSC. This could be related to the non-representation of landslides by the model, usually frequent in the basin, mainly in Suaçuí Grande, Santa Maria do Doce and Caratinga basins (PIRH, 2010). Another specific source that contributes to the increase in sediment load are those originating in mining (LOBO et al., 2016). That activity is historically present in the basin (HORA et al., 2012) and is carried out in several areas, primarily in the headwaters of the Carmo and Piracicaba rivers.

The reason to performed the experiment E7 (SSCbg) was the existence of some natural processes related to sediments that were not being represented by the model, which consequently was not adequately estimating SSC values during the dry season. This indicates that during the periods without precipitations, the Doce river have other sediment sources that aren't those originating in the hillslopes towards the channel. These sources could be the erosion of sediment bars (FRYIRS, 2013), erosion of the riverbed and the river banks (HOOKE, 2003) or even anthropogenic activities (LOBO et al., 2016). In the context of sediment transport connectivity, sediment bars (Figure 7) may have an important role in supplying the channel with sediments (FRYIRS, 2013). The largest part of these sediments corresponds to the fractions of silt and clay that, due to the large amount in the basin (LIMA et al., 2005), may be partly deposited during the rainy season and remain stored among the pores of sandbars. During the dry season, these fine sediments may be mobilized by flows with low SSC. Hooke (2003) mentions that a stable river downstream segment is more active, although coarse materials are not enough to supply the suspended sediment deficit, which causes fine sediments to be eroded from river banks. Coarse loads are transported especially for high water discharges, while transport of fine loads decreases proportionally (LIN et al., 2017).

The MGB-SED model and its structure

According to Morgan (2005), hardship in obtaining an exact adjustment between observed and calculated data reflects the uncertainty of the predictions performed by models. The author remarks that uncertainties originate from (i) errors in measured values; (ii) high spatial variability of some input parameters that could not be properly represented by a single value; (iii) the need to estimate some parameter values that cannot be easily measured; and (iv) errors in the model structure or the operating equations,
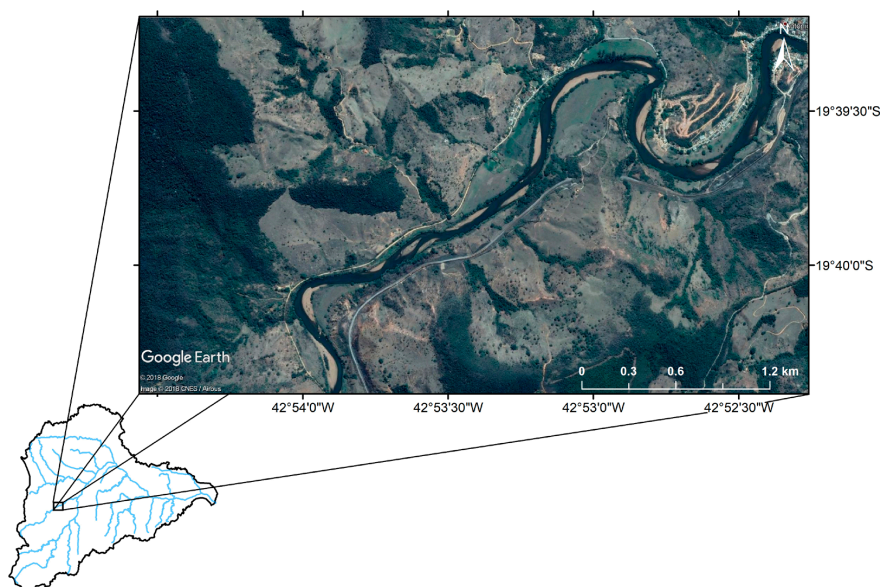
Figure 7. Sediment bars in Piracicaba River, a tributary of Doce River. Image from Oct. 19th, 2017. Source: Google Earth (2018).

particularly where empirical equations are not used to describe physical processes. At a deeper analysis level, the author mentions that there is still considerable uncertainty even regarding the nature of the mechanisms involved in soil particle detachment through surface runoff.

Oliveira and Quaresma (2017), while analyzing the 56994500 (Colatina) fluviometric station (~88% of the Doce river basin drainage area), concluded that 63% of the variation in suspended sediment load within the Doce River basin can be explained by runoff, and the remaining 37%, by other factors, such as rain intensity, vegetation cover and soil use. Rainfall, considered one of the main forcing in sediment models, also has great uncertainty in its measurements (XUE; CHEN; WU, 2014). In MGB-SED, rainfall values are interpolated to unit catchments centroids, which may lead rainfall values to be sometimes underestimated and, sometimes overestimated. Besides that, in the MUSLE equation, rain intensity factors are replaced by surface runoff and a peak flow to represent the maximum runoff energy acting over the soil. However, peak flow values are difficult to estimate (KINNELL; RISSE, 1998), and therefore a simplified assessment were performed in the MGB-SED.

It is known that MUSLE is an empirical equation that mathematically represents a power function, presenting a simple way to represent all the complexity of sedimentological processes. Sediment retention/deposition processes in landscape are not represented by a specific mathematical formulation, but are taken account in the equation (WILLIAMS, 1975). Shen, Chen and Chen (2012) in performing a SWAT model uncertainty analysis, which also employed MUSLE, demonstrated that the analysis of sediment simulations presented higher uncertainty than that of water discharge, and that uncertainty becomes even higher during rainy seasons. According to the authors, this could be related to the dependence that the sediment model has on the hydrological model.

It is practically unavoidable that there are uncertainties in the model parameters (SHEN; CHEN; CHEN, 2012). Hence, many model users tend to overcome uncertainty issues at the input parameters, splitting an observed data series into two periods, one for calibration and another for validation. However, calibration may not solve all uncertainty issues in modelling context, for it cannot be generalized for all environmental conditions (MORGAN, 2005) and the model parameters have acceptable ranges of values so that they may maintain their function.

CONCLUSIONS

Several automatic calibration and validation experiments for the MGB-SED model were performed using suspended sediment concentration (SSC), spectral surface reflectance (SSR) in the red band, turbidity and total suspended solids (TSS). We sought to investigate the applicability of surrogate data sources in the calibration and validation for a large-scale sediment model, given the scarcity of observed SSC data. Model calibration and validation procedures were carried out, using in each one, independent data for a given period. According to the literature research, this is one of the first studies to adopt this kind of approach.

After performed 37 automatic calibration and 111 validation tests, the main conclusions were:

- SSR, turbidity and TSS data have the potential to enhance the performance of the MGB-SED model. Generally, after MGB-SED calibration, the model performance was improved, with positive changes in correlation values. During validation, the model performance was generally poorer than that of calibration;

- From surrogate data used in this study, the best results in the calibration process were for experiments E2 and E3 (that used of 5 and 17 sub-basins, respectively) in which the correlation average was increased to 0.12 in SSR. On the

other hand, traditional SSC data showed the best result in experiment E10, where the ENS coefficient increased from -0.44 to 0.44 at the Fazenda Ouro Fino station. This station was the one that have the highest number of observed SSC data and highlight the importance of using in situ measured data together with a high sampling frequency, even when SSR data was available.

In summary, the results indicate that in basins devoid of in situ measurements, remote sensing data may be a powerful alternative in calibration and validation processes, enhancing the large-scale sediment model performance.

Furthermore, the performed experiments and the comparisons between observed and simulated data allowed to identify opportunities for improvements in the sediment model structure. To try fully represent what happens in environment, new processes should be included in the MGB-SED model. These enhancements will be the goal of future studies.

ACKNOWLEDGEMENTS

REFERENCES

ALLASIA, D. G.; SILVA, B.; COLLISCHONN, W.; TUCCI, C. E. M. Use of large basin simulation model MGB-IPH in Brazil. In: IAHS SCIENTIFIC ASSEMBLY, 7., 2015, Foz do Iguaçu. *Proceedings…* Oxfordshire: IAHS-AISH Publication, 2015.

ANA – AGÊNCIA NACIONAL DE ÁGUAS. *Encarte especial sobre a bacia do rio Doce:* rompimento da barragem em Mariana/MG. Brasília: ANA, 2016. Available from: http://arquivos.ana.gov.br/RioDoce/EncarteRioDoce_22_03_2016v2.pdf>. Access on: 14 dec. 2016.

ASTM – ASTM INTERNATIONAL. *D1889-00:* standard test method for turbidity of water. Philadelphia, 2003. (Water Environmental Technology, 11.01).

AYELE, G. T.; TESHALE, E. Z.; YU, B.; RUTHERFURD, I. D.; JEONG, J. Streamflow and sediment yield prediction for watershed prioritization in the Upper Blue Nile River Basin, Ethiopia. *Water (Basel)*, v. 9, n. 10, p. 782, 2017. http://dx.doi.org/10.3390/w9100782.

BEKELE, E. G.; NICKLOW, J. W. Multi-objective automatic calibration of SWAT using NSGA-II. *Journal of Hydrology (Amsterdam)*, v. 341, n. 3-4, p. 165-176, 2007. http://dx.doi.org/10.1016/j.jhydrol.2007.05.014.

BETRIE, G. D.; VAN GRIENSVEN, A.; MOHAMED, Y. A.; POPESCU, I.; MYNETT, A. E.; HUMMEL, S. Linking SWAT and SOBEK using open modeling interface (OPENMI) for sediment transport simulation in the Blue Nile River basin. *Transactions of the ASABE*, v. 54, n. 5, p. 1749-1757, 2011. http://dx.doi.org/10.13031/2013.39847.

BEZAK, N.; RUSJAN, S.; PETAN, S.; SODNIK, J.; MIKOŠ, M. Estimation of soil loss by the WATEM/SEDEM model using an automatic parameter estimation procedure. *Environmental Earth Sciences*, v. 74, n. 6, p. 5245-5261, 2015. http://dx.doi.org/10.1007/s12665-015-4534-0.

BLASONE, R. S.; MADSEN, H.; ROSBJERG, D. Parameter estimation in distributed hydrological modelling: comparison of global and local optimisation techniques. *Hydrology Research*, v. 38, n. 4-5, p. 451-476, 2007. http://dx.doi.org/10.2166/nh.2007.024.

BOITEN, W. *Hydrometry:* IHE delft lecture note series. USA: CRC Press, 2008.

BOYLE, D. P.; GUPTA, H. V.; SOROOSHIAN, S. Toward improved calibration of hydrologic models: Combining the strengths of manual and automatic methods. *Water Resources Research*, v. 36, n. 12, p. 3663-3674, 2000. http://dx.doi.org/10.1029/2000WR900207.

BRESSIANI, D. A.; GASSMAN, P. W.; FERNANDES, J. G.; GARBOSSA, L. H. P.; SRINIVASAN, R.; BONUMÁ, N. B.; MENDIONDO, E. M. A review of soil and water assessment tool (SWAT) applications in Brazil: Challenges and prospects. *International Journal of Agricultural and Biological Engineering*, v. 8, n. 3, p. 1-27, 2015. Available from: <http://www.scopus.com/inward/record.url?eid=2-s2.0-84935036175&partnerID=tZOtx3y1>. Access on: 30 july 2018.

BUARQUE, D. C. *Simulação da geração e do transporte de sedimentos em grandes bacias:* estudo de caso do rio madeira. 2015, 182 f. Tese (Doutorado em Recursos Hídricos e Saneamento Ambiental) – Instituto de Pesquisas Hidráulicas, Universidade Federal do Rio Grande do Sul, Porto Alegre, 2015.

BUSSI, G.; FRANCÉS, F.; MONTOYA, J. J.; JULIEN, P. Y. Distributed sediment yield modelling: importance of initial sediment conditions. *Environmental Modelling & Software*, v. 58, p. 58-70, 2014. https://doi.org/10.1016/j.envsoft.2014.04.010.

COLLISCHONN, W.; ALLASIA, D.; SILVA, B. C.; TUCCI, C. E. M. The MGB-IPH model for large-scale rainfall—runoff modelling. *Hydrological Sciences Journal*, v. 52, n. 5, p. 878-895, 2007. http://dx.doi.org/10.1623/hysj.52.5.878.

COLLISCHONN, W.; TUCCI, C. E. M. Ajuste multiobjetivo dos parâmetros de um modelo hidrológico. *Revista Brasileira de Recursos Hídricos*, v. 8, n. 3, p. 27-39, 2003. http://dx.doi.org/10.21168/rbrh.v8n3.p27-39.

DESMET, P. J. J.; GOVERS, G. A GIS-procedure for automatically calculating the USLE LS-factor on topographically complex landscape units. *Journal of Soil and Water Conservation*, v. 51, n. 5, p. 427-433, 1996.

ELSEL, D. R.; HIRSCH, R. M. *Statistical methods in water resources.* USA: Elsevier, 1992.

ESPINOZA VILLAR, R.; MARTINEZ, J.-M.; GUYOT, J.-L.; FRAIZY, P.; ARMIJOS, E.; CRAVE, A.; BAZÁN, H.; VAUCHEL, P.; LAVADO, W. The integration of field measurements and satellite observations to determine river solid loads in poorly monitored basins. *Journal of Hydrology (Amsterdam)*, v. 444, p. 221-228, 2012. http://dx.doi.org/10.1016/j.jhydrol.2012.04.024.

FAGUNDES, H. O.; FAN, F. M.; PAIVA, R. C. D.; BUARQUE, D. C. Simulação hidrossedimentológica preliminar na Bacia do Rio Doce com o Modelo MGB-SED. In: CONGRESSO INTERNACIONAL DE HIDROSSEDIMENTOLOGIA, 2., 2017, Foz do Iguaçu. *Anais...* Porto Alegre: ABRH, 2017.

FAGUNDES, H. O.; PAIVA, R. C. D.; FAN, F. M. Sedimentos em suspensão observados com imagens Landsat para modelagem de grandes bacias. In: SIMPÓSIO BRASILEIRO DE RECURSOS HÍDRICOS, 22., 2017, Florianópolis. *Anais...* Porto Alegre: ABRH, 2017.

FAN, F. M.; BUARQUE, D. C.; PONTES, P. R. M.; COLLISCHONN, W. Um mapa de unidades de resposta hidrológica para a América do Sul. In: SIMPÓSIO BRASILEIRO E RECURSOS HÍDRICOS, 21., 2015, Brasília. *Anais...* Porto Alegre: ABRH, 2015a.

FAN, F. M.; COLLISCHONN, W. Integração do Modelo MGB-IPH com Sistema de Informação Geográfica. *Revista Brasileira de Recursos Hídricos*, v. 19, n. 1, p. 243-254, 2014. http://dx.doi.org/10.21168/rbrh.v19n1.p243-254.

FAN, F. M.; COLLISCHONN, W.; QUIROZ, K. J.; SORRIBAS, M. V.; BUARQUE, D. C.; SIQUEIRA, V. A. Flood forecasting on the Tocantins River using ensemble rainfall forecasts and real-time satellite rainfall estimates. *Journal of Flood Risk Management*, v. 9, n. 3, p. 278-288, 2016. http://dx.doi.org/10.1111/jfr3.12177.

FAN, F. M.; SCHWANENBERG, D.; COLLISCHONN, W.; WEERTS, A. Verification of inflow into hydropower reservoirs using ensemble forecasts of the TIGGE database for large scale basins in Brazil. *Journal of Hydrology:* Regional Studies, v. 4, p. 196-227, 2015b.

FAO – FOOD AND AGRICULTURE ORGANIZATION OF THE UNITED NATIONS. *Soil map of the world.* Rome: FAO, 1971. v. 4.

FRYIRS, K. (Dis) Connectivity in catchment sediment cascades: a fresh look at the sediment delivery problem. *Earth Surface Processes and Landforms*, v. 38, n. 1, p. 30-46, 2013. http://dx.doi.org/10.1002/esp.3242.

GETIRANA, A. C. V.; BONNET, M.-P.; ROTUNNO FILHO, O. C.; COLLISCHONN, W.; GUYOT, J.-L.; SEYLER, F.; MANSUR, W. J. Hydrological modelling and water balance of the Negro River basin: evaluation based on in situ and spatial altimetry data. *Hydrological Processes*, v. 24, n. 22, p. 3219-3236, 2010. https://doi.org/10.1002/hyp.7747.

GLYSSON, G. D.; GRAY, J. R.; CONGE, L. M. Adjustment of total suspended solids data for use in sediment studies. In: ASCE'S 2000 JOINT CONFERENCE ON WATER RESOURCES ENGINEERING AND WATER-RESOURCES PLANNING AND MANAGEMENT, 2000, Minneapolis, Minn. *Proceedings…* Reston: ASCE, 2000. 10 p. http://dx.doi.org/10.1061/40517(2000)270.

GOOGLE EARTH. 2018. Available from: <https://www.google.com.br/intl/pt-BR/earth>. Access on: 05 Apr. 2019.

GUPTA, H. V.; KLING, H.; YILMAZ, K. K.; MARTINEZ, G. F. Decomposition of the mean squared error and NSE performance criteria: implications for improving hydrological modelling. *Journal of Hydrology (Amsterdam)*, v. 377, n. 1-2, p. 80-91, 2009. http://dx.doi.org/10.1016/j.jhydrol.2009.08.003.

GUPTA, H. V.; SOROOSHIAN, S.; YAPO, P. O. Toward improved calibration of hydrologic models: multiple and noncommensurable measures of information. *Water Resources Research*, v. 34, n. 4, p. 751-763, 1998. http://dx.doi.org/10.1029/97WR03495.

HOOKE, J. Coarse sediment connectivity in river channel systems: a conceptual framework and methodology. *Geomorphology*, v. 56, n. 1-2, p. 79-94, 2003. http://dx.doi.org/10.1016/S0169-555X(03)00047-3.

HORA, A. M.; DIAS, C. A.; GUEDES, G. R.; COSTA, A. S. V.; FERRARI JUNIOR, M. J. *Território, mobilidade populacional e ambiente:* da exploração econômica da bacia hidrográfica do Rio Doce ao atual processo de degradação de seus recursos naturais. Governador Valadares: Editora Univale, 2012. Available from: <http://gilvanguedes.com/wp-content/uploads/2016/09/hora_etal_2012_livro_tmpa_cap9.pdf>. Access on: 30 jan. 2018.

JENSEN, J. R. *Sensoriamento remoto do ambiente:* uma perspectiva em recursos terrestres. São José dos Campos: Parênteses, 2009. p. 598.

KINNELL, P.; RISSE, L. USLE-M: empirical modelling rainfall erosion through runoff and sediment concentration. *Soil Science Society of America Journal*, v. 62, n. 6, p. 1667-1672, 1998. http://dx.doi.org/10.2136/sssaj1998.03615995006200060026x.

LIMA, J. E. F. W.; LOPES, W. T. A.; CARVALHO, N. O.; VIEIRA, M. R.; SILVA, E. M. Suspended sediment fluxes in the large river basins of Brazil. In: SYMPOSIUM OF THE SEDIMENT BUDGETS 1 & 2, 7., 2005, Foz do Iguaçu. *Proceedings…* Oxfordshire: IAHS-AISH Publication, 2005. p. 355-363.

LIN, J.; HUANG, Y.; ZHAO, G.; JIANG, F.; WANG, M. K.; GE, H. Flow-driven soil erosion processes and the size selectivity of eroded sediment on steep slopes using colluvial deposits in a permanent gully. *Catena*, v. 157, p. 47-57, 2017. http://dx.doi.org/10.1016/j.catena.2017.05.015.

LOBO, F. D. L.; COSTA, M.; NOVO, E. M. L. D. M.; TELMER, K. Distribution of artisanal and small-scale gold mining in the Tapajós River Basin (Brazilian Amazon) over the past 40 years

and relationship with water siltation. *Remote Sensing*, v. 8, n. 7, p. 579, 2016. http://dx.doi.org/10.3390/rs8070579.

LODHI, M. A.; RUNDQUIST, D. C.; HAN, L.; KUZILA, M. S. Estimation of suspended sediment concentration in water using integrated surface reflectance. *Geocarto International*, v. 13, n. 2, p. 11-15, 1998. http://dx.doi.org/10.1080/10106049809354637.

MARTINEZ, J. M.; GUYOT, J. L.; FILIZOLA, N.; SONDAG, F. Increase in suspended sediment yield of the Amazon river assessed by monitoring network and satellite data. *Catena*, v. 79, n. 3, p. 257-264, 2009. http://dx.doi.org/10.1016/j.catena.2009.05.011.

MARTINS, V. S.; BARBOSA, C. C. F.; CARVALHO, L. A. S.; JORGE, D. S. F.; LOBO, F. D. L.; NOVO, E. M. L. D. M. Assessment of atmospheric correction methods for Sentinel-2 MSI images applied to Amazon floodplain lakes. *Remote Sensing*, v. 9, n. 4, p. 322, 2017. http://dx.doi.org/10.3390/rs9040322.

MERRITT, W. S.; LETCHER, R. A.; JAKEMAN, A. J. A review of erosion and sediment transport models. *Environmental Modelling & Software*, v. 18, n. 8-9, p. 761-799, 2003. http://dx.doi.org/10.1016/S1364-8152(03)00078-1.

MILLER, R. L.; DEL CASTILLO, C. E.; CHILMAKURI, C.; MCCORQUODALE, J. A.; GEORGIOU, I.; MCKEE, B. A.; D'SA, E. J. Using multi-temporal MODIS 250 m data to calibrate and validate a sediment transport model for environmental monitoring of coastal waters. In: INTERNATIONAL WORKSHOP ON THE ANALYSIS OF MULTI-TEMPORAL REMOTE SENSING IMAGES, 2005, Biloxi. USA: IEEE, 2005. p. 200-204. http://dx.doi.org/10.1109/AMTRSI.2005.1469872.

MILLINGTON, A. C. Reconnaissance scale soil erosion mapping using a simple geographic information system in the humid tropics. In: SIDERIUS, W. (Ed.). *Land evaluation for land-use planning and conservation in sloping areas*. Wageningen: ILRI, 1986. p. 64-81.

MINELLA, J. P.; MERTEN, G. H.; REICHERT, J. M.; CLARKE, R. T. Estimating suspended sediment concentrations from turbidity measurements and the calibration problem. *Hydrological Processes*, v. 22, n. 12, p. 1819-1830, 2008. http://dx.doi.org/10.1002/hyp.6763.

MORGAN, R. P. C. *Soil erosion & conservation*. 3rd ed. Oxford: Blackwell Publishing, 2005.

MORIASI, D. N.; ARNOLD, J. G.; VAN LIEW, M. W.; BINGNER, R. L.; HARMEL, R. D.; VEITH, T. L. Model evaluation guidelines for systematic quantification of accuracy in watershed simulations. *Transactions of the ASABE*, v. 50, n. 3, p. 885-900, 2007. http://dx.doi.org/10.13031/2013.23153.

MORRIS, G. L.; FAN, J. *Reservoir sedimentation*. New York: McGraw-Hill Book Co., 1998.

MULETA, M. K.; NICKLOW, J. W. Sensitivity and uncertainty analysis coupled with automatic calibration for a distributed

watershed model. *Journal of Hydrology (Amsterdam)*, v. 306, n. 1-4, p. 127-145, 2005. http://dx.doi.org/10.1016/j.jhydrol.2004.09.005.

MUNDAY JUNIOR, J. C.; ALFÖLDI, T. T. Landsat test of diffuse reflectance models for aquatic suspended solids measurement. *Remote Sensing of Environment*, v. 8, n. 2, p. 169-183, 1979. http://dx.doi.org/10.1016/0034-4257(79)90015-4.

NASH, J. E.; SUTCLIFFE, J. V. River flow forecasting through conceptual models part I - A discussion of principles. *Journal of Hydrology (Amsterdam)*, v. 10, n. 3, p. 282-290, 1970. http://dx.doi.org/10.1016/0022-1694(70)90255-6.

NÓBREGA, M. T.; COLLISCHONN, W.; TUCCI, C. E. M.; PAZ, A. R. Uncertainty in climate change impacts on water resources in the Rio Grande Basin, Brazil. *Hydrology and Earth System Sciences*, v. 15, n. 2, p. 585-595, 2011. http://dx.doi.org/10.5194/hess-15-585-2011.

OLIVEIRA, K. S. S.; QUARESMA, V. S. Temporal variability in the suspended sediment load and streamflow of the Doce River. *Journal of South American Earth Sciences*, v. 78, p. 101-115, 2017. http://dx.doi.org/10.1016/j.jsames.2017.06.009.

OP DE HIPT, F.; DIEKKRÜGER, B.; STEUP, G.; YIRA, Y.; HOFFMANN, T.; RODE, M. Applying SHETRAN in a Tropical West African Catchment (Dano, Burkina Faso) -calibration, validation, uncertainty assessment. *Water (Basel)*, v. 9, n. 2, p. 101, 2017. http://dx.doi.org/10.3390/w9020101.

PANDEY, A.; HIMANSHU, S. K.; MISHRA, S. K.; SINGH, V. P. *Catena Physically based soil erosion and sediment yield models revisited*. Catena: Elsevier B.V., 2016. v. 147, p. 595-620. http://dx.doi.org/10.1016/j.catena.2016.08.002.

PAVANELLI, D.; BIGI, A. Indirect methods to estimate suspended sediment concentration: reliability and relationship of turbidity and settleable solids. *Biosystems Engineering*, v. 90, n. 1, p. 75-83, 2005. http://dx.doi.org/10.1016/j.biosystemseng.2004.09.001.

PINTO, W. D. P.; LIMA, G. B.; ZANETTI, J. B. Análise comparativa de modelos de séries temporais para modelagem e previsão de regimes de vazões médias mensais do Rio Doce, Colatina - Espírito Santo. *Ciência e Natura*, v. 37, n. 3, p. 1-11, 2015. http://dx.doi.org/10.5902/2179460X17143.

PIRH – BACIA DO RIO DOCE. *Plano Integrado de Recursos Hídricos da Bacia Hidrográfica do Rio Doce*. Porto Alegre: Consórcio Ecoplan-Lume, 2010. v. 1. Relatório Final.

REFSGAARD, J. C. Parameterisation, calibration and validation of distributed hydrological models. *Journal of Hydrology (Amsterdam)*, v. 198, n. 1-4, p. 69-97, 1997. http://dx.doi.org/10.1016/S0022-1694(96)03329-X.

ROSTAMIAN, R.; JALEH, A.; AFYUNI, M.; MOUSAVI, S. F.; HEIDARPOUR, M.; JALALIAN, A.; ABBASPOUR, K. C. Application of a SWAT model for estimating runoff and sediment

in two mountainous basins in central Iran. *Hydrological Sciences Journal*, v. 53, n. 5, p. 977-988, 2008. http://dx.doi.org/10.1623/hysj.53.5.977.

SADEGHI, S. H. R.; GHOLAMI, L.; KHALEDI DARVISHAN, A.; SAEIDI, P. A review of the application of the MUSLE model worldwide. *Hydrological Sciences Journal*, v. 59, n. 2, p. 365-375, 2014. http://dx.doi.org/10.1080/02626667.2013.866239.

SANTOS, C. A. G.; PINTO, L. E. M.; FREIRE, P. K. M. M.; MISHRA, S. K. Application of a particle swarm optimization to a physically-based erosion model. *Annals of Warsaw University of Life Sciences – SGGW. Land Reclamation*, v. 42, n. 1, p. 39-49, 2010. http://dx.doi.org/10.2478/v10060-008-0063-9.

SANTOS, C. A. G.; SRINIVASAN, V. S.; SUZUKI, K.; WATANABE, M. Application of an optimization technique to a physically based erosion model. *Hydrological Processes*, v. 17, n. 5, p. 989-1003, 2003. http://dx.doi.org/10.1002/hyp.1176.

SANTOS, L. L. Modelos hidráulicos-hidrológicos: conceitos e aplicações. *Revista Brasileira de Geografia Física*, v. 2, p. 1-19, 2009.

SARI, V.; CASTRO, N. M. R.; PEDROLLO, O. C. Estimate of suspended sediment concentration from monitored data of turbidity and water level using artificial neural networks. *Water Resources Management*, v. 31, n. 15, p. 4909-4923, 2017. http://dx.doi.org/10.1007/s11269-017-1785-4.

SHEN, Z. Y.; CHEN, L.; CHEN, T. Analysis of parameter uncertainty in hydrological and sediment modeling using GLUE method: a case study of SWAT model applied to Three Gorges Reservoir Region, China. *Hydrology and Earth System Sciences*, v. 16, n. 1, p. 121-132, 2012. http://dx.doi.org/10.5194/hess-16-121-2012.

SINGH, A.; IMTIYAZ, M.; ISAAC, R. K.; DENIS, D. M. Assessing the performance and uncertainty analysis of the SWAT and RBNN models for simulation of sediment yield in the Nagwa watershed, India. *Hydrological Sciences Journal*, v. 59, n. 2, p. 351-364, 2014. http://dx.doi.org/10.1080/02626667.2013.872787.

SOROOSHIAN, S.; GUPTA, V. K. Model calibration In: SINGH, V. J. (Ed.). *Computer models of watershed hydrology*. Highlands Ranch: Water Resourc. Pub., 1995. 1130 p.

STEWART, J.; RAJAGOPALAN, B.; KASPRZYK, J.; RASEMAN, W.; LIVNEH, B. The use of ensemble modeling of suspended sediment to characterize uncertainty. In: WORLD ENVIRONMENTAL AND WATER RESOURCES CONGRESS, 2017, California. *Proceedings…* Reston: ASCE, 2017. p. 207-218. http://dx.doi.org/10.1061/9780784480625.019.

SUGAWARA, M. Automatic calibration of the tank model/L'étalonnage automatique d'un modèle à cisterne. *Hydrological Sciences Journal*, v. 24, n. 3, p. 375-388, 1979. http://dx.doi.org/10.1080/02626667909491876.

TUCCI, C. E. M.; COLLISCHONN, W. Ajuste multi-objetivo dos parâmetros de um modelo hidrológico. *Revista Brasileira de Recursos Hídricos*, v. 8, n. 3, p. 27-39, 2003. http://dx.doi.org/10.21168/rbrh.v8n3.p27-39.

TUCCI, C.; BRAVO, J.; COLLISCHONN, W. Verificação da eficiência e eficácia de um algoritmo evolucionário multi-objetivo na calibração automática do modelo hidrológico IPH II. *Revista Brasileira de Recursos Hídricos*, v. 14, n. 3, p. 37-50, 2009. http://dx.doi.org/10.21168/rbrh.v14n3.p37-50.

USGS – UNITED STATES GEOLOGICAL SURVEY. *EarthExplorer – Home*. USA: USGS, 2018a. Available from: <https://earthexplorer.usgs.gov>. Access on: 5 Apr. 2019.

USGS – UNITED STATES GEOLOGICAL SURVEY. *Product Guide:* LandsaT 4-7 surface reflectance (LEDAPS) product guide. USA: USGS, 2018b. Available from: <https://prd-wret.s3-us-west-2.amazonaws.com/assets/palladium/production/s3fs-public/atoms/files/LSDS-1370_L4-7_Surface%20Reflectance-LEDAPS-Product-Guide.pdf>. Access on: 05 Apr. 2019.

VAN ROMPAEY, A.; BAZZOFFI, P.; JONES, R. J.; MONTANARELLA, L. Modeling sediment yields in Italian catchments. *Geomorphology*, v. 65, n. 1-2, p. 157-169, 2005. http://dx.doi.org/10.1016/j.geomorph.2004.08.006.

VINEY, N. R.; SIVAPALAN, M. A conceptual model of sediment transport: application to the Avon River Basin in Western Australia. *Hydrological Processes*, v. 13, n. 5, apr. 1999, p. 727-743. http://dx.doi.org/10.1002/(SICI)1099-1085(19990415)13:5<727::AID-HYP776>3.0.CO;2-D.

VRUGT, J.A.; GUPTA, H.V.; BOUTEN, W.; SOROOSHIAN, S. A Shuffled Complex Evolution Metropolis algorithm for optimization and uncertainty assessment of Hydrologic model parameters. *Water Resources Research*, v. 39, n. 8, p. 1-18, 2003. http://dx.doi.org/10.1029/2002WR001642.

WANG, J. J.; LU, X. X.; LIEW, S. C.; ZHOU, Y. Retrieval of suspended sediment concentrations in large turbid rivers using Landsat ETM+: an example from the Yangtze River, China. *Earth Surface Processes and Landforms*, v. 34, n. 8, p. 1082-1092, 2009. http://dx.doi.org/10.1002/esp.1795.

WANG, X.; MOSLEY, C. T.; FRANKENBERGER, J. R.; KLADIVKO, E. J. Subsurface drain flow and crop yield predictions for different drain spacings using DRAINMOD. *Agricultural Water Management*, v. 79, n. 2, p. 113-136, 2006. https://doi.org/10.1016/j.agwat.2005.02.002.

WILLIAMS, J. R. Sediment-yield prediction with universal equation using runoff energy factor. In: SEDIMENT-YIELD WORKSHOP, 1975, Oxford. *Proceedings…* Oxford: USDA Sedimentation Laboratory, 1975.

WILLIAMS, J. R. The EPIC model. In: SINGH, V. P. *Computer models of watershed hydrology*. Highlands Ranch: Water Resources Publications, 1995. p. 909-1000. Chap. 25.

WILLIAMSON, T. N.; CRAWFORD, C. G. Estimation of suspended-sediment concentration from total suspended solids and turbidity data for Kentucky, 1978-1995. *JAWRA Journal of the American Water Resources Association*, v. 47, n. 4, p. 739-749, 2011. http://dx.doi.org/10.1111/j.1752-1688.2011.00538.x.

WISCHMEIER, W. H.; SMITH, D. D. *Predicting rainfall erosion losses* – a guide to conservation planning. USA: U. S. Department of Agriculture, 1978. (Agriculture handbook, 537).

WORKU, T.; KHARE, D.; TRIPATHI, S. K. Modeling runoff–sediment response to land use/land cover changes using integrated GIS and SWAT model in the Beressa watershed. *Environmental Earth Sciences*, v. 76, n. 16, p. 550, 2017. http://dx.doi.org/10.1007/s12665-017-6883-3.

XUE, C.; CHEN, B.; WU, H. Parameter uncertainty analysis of surface flow and sediment yield in the Huolin Basin, China. *Journal of Hydrologic Engineering*, v. 19, n. 6, p. 1224-1236, 2014. http://dx.doi.org/10.1061/(ASCE)HE.1943-5584.0000909.

YANG, X.; MAO, Z.; HUANG, H.; WANG, T.; LIU, D. Numerical simulation of suspended sediment transport merging with satellite derived data in coastal waters. In: *SPIE ASIA-PACIFIC REMOTE SENSING*, 2014, China. Bellingham: International Society for Optics and Photonics, 2014. p. 92650E-92650E-8.

YAPO, P. O.; GUPTA, H. V.; SOROOSHIAN, S. Multi-objective global optimization for hydrologic models. *Journal of Hydrology (Amsterdam)*, v. 204, n. 1-4, p. 83-97, 1998. http://dx.doi.org/10.1016/S0022-1694(97)00107-8.

YEN, H.; LU, S.; FENG, Q.; WANG, R.; GAO, J.; BRADY, D. M.; SHARIFI, A.; AHN, J.; CHEN, S. T.; JEONG, J.; WHITE, M. J.; ARNOLD, J. G. Assessment of optional sediment transport functions via the complex watershed simulation model SWAT.

Water (Basel), v. 9, n. 2, p. 76, 2017. http://dx.doi.org/10.3390/w9020076.

YESUF, H. M.; ASSEN, M.; ALAMIREW, T.; MELESSE, A. M. Modeling of sediment yield in Maybar gauged watershed using SWAT, northeast Ethiopia. *Catena*, v. 127, p. 191-205, 2015. http://dx.doi.org/10.1016/j.catena.2014.12.032.

YIN, L.; WANG, X.; PAN, J.; GASSMAN, P. W. Evaluation of APEX for daily runoff and sediment yield from three plots in the Middle Huaihe River Watershed, China. *Transactions of the ASABE*, v. 52, n. 6, p. 1833-1845, 2009. http://dx.doi.org/10.13031/2013.29212.

ZHANG, M.; DONG, Q.; CUI, T.; XUE, C.; ZHANG, S. Suspended sediment monitoring and assessment for Yellow River estuary from Landsat TM and ETM+ imagery. *Remote Sensing of Environment*, v. 146, p. 136-147, 2014. http://dx.doi.org/10.1016/j.rse.2013.09.033.

Authors contributions

Hugo de Oliveira Fagundes: The author performed the calibration and validation experiments and worked on the manuscript writing.

Fernando Mainardi Fan: The author assisted the experimental delineation and revised the manuscript.

Rodrigo Cauduro Dias de Paiva: The author assisted the experimental delineation and revised the manuscript.

SUPPLEMENTARY MATERIAL

Supplementary material accompanies this paper.
Legend S1. MGB-SED calibration parameters for the Doce river basin.
This material is available as part of the online article from http://www.scielo.br/rbrh